FUTURE PROSPECTS FOR HYPERSONIC FLIGHT TEST FOR UNIVERSITY STUDENTS

J.M.A. Longo[(1)],
Tel.: +49 531 295 2643 Fax: +49 531 295 2320 Email: Jose.Longo@dlr.de

O. Bozic et al.[(1)], J. Behrens et al. [(2)], P. Lehmann et al. [(3)]
[(1)]DLR, Lilienthalplatz 7, D-38108 Braunschweig, Germany
[(2)]EADS-ST, D-28361 Bremen, Germany
[(3)]ISL, F-68301 Saint-Louis Cedex, France

Abstract

The transport to space of satellites and experiments with conventional expandable rockets is a very expensive and time demanding business and therefore almost prohibitive for Universities and High-School or Colleges laboratories. In this lecture an unconventional, low-cost reusable concept-system based on "electromagnetic railgun" is presented and discussed. The aims is to provide in the midterm with a system capable of launch in LEO small satellites of maximum 5 kg weight not by using conventional chemical power but accelerating them up to hypersonic speed with help of electromagnetic forces. In the short term such system could offer the possibility to carry out low-cost hypersonic- and atmospheric-research experiments. The subject of the lecture is to demonstrate the feasibility of launching small meteorological science experiment-payloads by means of hypersonic projectiles, which are accelerated with an electromagnetic railgun up to an end-velocity of about 2100m/s. Associated with this new non-conventional propulsion technique is the development of hypersonic projectiles which shall withstand a harsh thermo-mechanical environment resulting from accelerations of about 10,000g. Compared to the solid and/or liquid rockets available today, a railgun launcher concept-system offers several advantages such as high efficiency with high repetitions rates and low recurring costs than today's market prices.

1. Introduction

Conventional rockets are driven by the combustion of liquid and/or solid chemicals, a propellant and an oxidizer, which are carried onboard the rocket. Fundamental to their propulsion is the conversion of thermal energy into kinetic energy by an adiabatic expansion. The speed and acceleration of the rockets is relatively small after lift-off, but they are continuously increased over a longer time period until the rocket reaches the required end-velocity. The disadvantage of all staged rockets employed so far is the non-reusability and the very small ratio between payload and fuel mass, which is in general less than 1% of the lift-off mass. To overcome these constraints, worldwide efforts are underway to establish programs for commercially competitive reusable engines and rockets. However, the ratio of the payload to take-off-mass of these new launch vehicles will be even worse. By employing a new propulsion technique, based upon a so-called railgun which uses electromagnetic forces for the acceleration of projectiles, the major disadvantages of the conventional rockets can be overcome and a reusability of the entire propulsion part as well as an improved ratio of payload to take-off-mass can be achieved. Only the projectile and some minor support structures are the expendable parts of the system. Indeed, railguns are well-known for their

capability to reach very high velocities (v_0 > 2000 m/s) with overall efficiencies (Ecinetic/Eeletric) over 30 %. The expected high performance concerning velocity, efficiency, cost and repetition rates make this system attractive not only for military but also for space applications [1]. A launch price is envisaged which is drastically lower per kilo than today's market prices for conventional rockets. Indeed, the idea to launch rockets with one single shot, as described by Jules Vernes in his novel “From the Earth to the Moon” appears to become realistic and will be here addressed.

The general system-principles have already been investigated by EADS Space Transportation (formerly Dasa) under an ESA Contract 13420/99/NL/MV [2]. The investigation has confirmed the idea, functions and criteria of launching payloads as a complement to conventional rocket systems. In that study the main focus was the return of probes from ISS to Earth and/or the launch of micro-satellites with a launch mass of about 100 kg into LEO. Two further studies, mostly dealing with the theoretical background of a railgun launch, have been performed additionally in the past [3-4]. However, no further actions have been pursued after the finalization of these studies. Here it is recall the attention on the usage of the railgun technology for the launch of small payloads to sub-orbital altitudes. The realization and validation of such launcher is considered as a stepping stone for a future envisaged launch of small satellites (~5 kg) into Low Earth Orbit. While these applications are considered realistic to be implemented based upon a "reasonable" extension of the existing railgun technology available in Europe, this launch system will be in position to provide flights at cost which are considerably lower than today's conventional rockets. Furthermore, in general there are further supplementary fields for a railgun application worth to consider as for instance as hypersonic test bed for new materials and/or new hypersonic re-entry concepts.

In the following chapters is discussed a concept being now realized by EADS Space Transportation [5] for launch scientific experiments into suborbital altitudes, permitting to test out and validate all basic features of this new system in a smaller scale.

2. Concept

During the time period 1955-1970 a lot of experiments with experimental projectiles launched with classical powder guns were performed. Remarkable from that period is the High Altitude Research Program (HARP) [6] with the big 16 inch gun system able to launch test probes into the upper atmosphere. Before HARP small portable gun launchers were used for the same purpose and even during HARP hundreds of high altitude flights were conducted using small guns. Some of the most notorious launch systems conceived during the HARP Program are the 5 and 7 inch gun-launch systems. The 5 inch gun-launch system, initially designed to satisfy the requirements of the Meteorological Rocket Network, required that a 0.9 kg (2 lb) payload be carried to an altitude of 65 km (40 miles). Typical payloads were a radar reflective chaff ejected at apogee, which was tracked by a radar to yield wind data and a small meteorological sounds which drifted to earth under large parachutes and returned radio telemetry of temperature and humidity. The 7 inch gun-launch system (**Fig. 1**), which represented the 5 inch system scaled up to the largest practicable barrel size while still remaining portable, was created by smooth boring a 175 mm gun and extending it in a similar manner as the 5 inch gun system. The completed gun barrel was 16.8 m (55 feet) long (7 inch L 92.4) and was installed in a modified T-76 mount. Two of the new

guns were constructed. The 7 inch guns had 3 times the payload capacity of the 5 inch guns and an altitude capability in excess of 100 km.

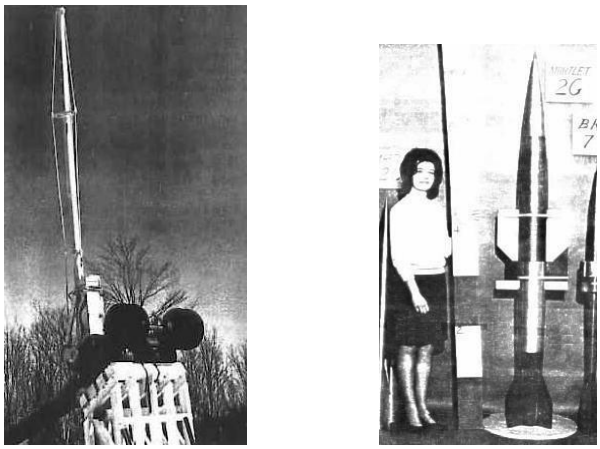

Figure 1: HARP-7 inch gun launcher (left). Martlet-2G projectile (right).

Also, the projectiles used in the HARP program are still today a technological challenger. Particularly to mention are the Martlet-2 and Martlet-3 series. The Martlet-2 series were used to conduct extensive researches at altitudes of up to 180 km with some 200 flights being conducted between 1963 and 1967. The Martlet-2 series were remarkably effective and reliable with a nearly perfect operational flight reliably record. The primary advantages of the Martlet-2 series were their versatility and their very low costs, about 3 thousands u$ per flight, which allowed hundreds of flights with a wide variety of payloads. The Martlet-3 series (**Fig. 2**) were the first serious attempt to produce a sub-calibre, gun-launched, rocket-assisted, vehicle for the 16 inch gun system. The basic design criteria for the Martlet-3 series was to gun launch a vehicle containing a rocket motor that could provide a velocity boost equal to or greater than the initial gun-launch velocity. The theoretical performance of the Martlet-3A was for a 18 kg payload to be carried to an altitude of some 500 km at gun-launch accelerations of 12-14,000 g's and gun launch velocities in the range of 2100 m/sec (similar to the Martlet-2 series maximum launch parameters).

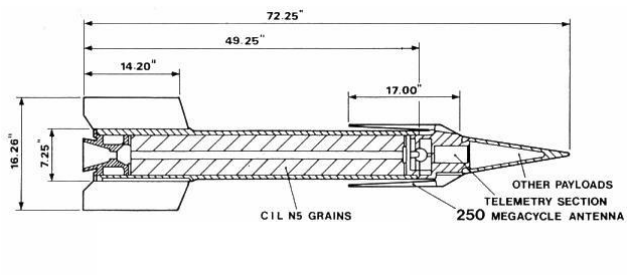

Figure 2: Sub-calibre Gun Fired Rocket Martlet-3A.

Furthermore, the technology of electromagnetic railguns is well known since the first experiments in France in the 1910's and up to date are primarily used in military research for the launch of high speed shells. The Institute Saint Louis (ISL) in France is presently with DSTL in UK the only European organization still working on electromagnetic railguns [7]. The physics of a railgun are not conceptually difficult. A current, flowing through rails and a conductive armature, which is free to slide, forms a closed loop, which in turn creates a magnetic field. This magnetic field generates a Lorentz force on the movable armature in an outward direction. The railgun takes advantage of this phenomenon and uses the Lorentz force to accelerate the armature and propel the projectile out of the gun barrel (**Fig. 3**).

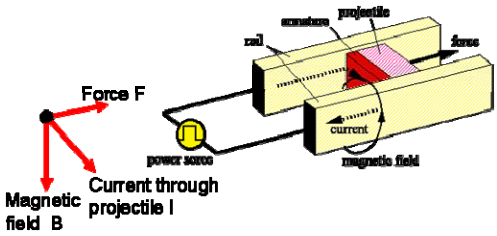

Figure 3: Railgun physical principle.

The kinetic energy of the projectile at the muzzle ranges from about 3 MJ for a 1 kg projectile with a velocity of 2500 m/s to 15 MJ (5 kg; 2500 m/s). For one single shot the electrical energy to be stored is between 9MJ and 45MJ, assuming an efficiency of 33%. Therefore, the power to be delivered to the railgun increases from 2 GW to 9 GW for a travel duration of the projectile in the barrel of about 5 ms. This energy is provided in the case of the ISL Pegasus facility (**Fig. 4**) by a modular 10 MJ capacitor bank, which consists of 200 individual modules of 50 kJ each; every module is made up of a fast discharge capacitor associated with a semiconductor switching system (10kV, 70kA), a coil and coaxial cable. To improve the efficiency of the railgun, a so-called "Distributed Energy Storage" (DES) is used, which delivers the energy along the rails. With such kind of railguns an overall efficiency of 30% to 40% is possible with muzzle velocities up to 3000 m/s. One example of the superimposed resulting current waveform generated by thirteen capacitor modules is shown in **Fig. 5**.

Figure 4: The ISL PEGASUS railgun facility.

The general operational capability for the railgun system will be demonstrated at first with the launch of small meteorological payloads to sub-orbital altitudes. These payloads which are launched today not by the above mentioned system but by very small sounding rockets have the advantage of restricted requirements with respect to mass, volume, target altitude and functionality. The design of the railgun and the associated hypersonic projectile will be tailored to the launch of these lightweight experiments.

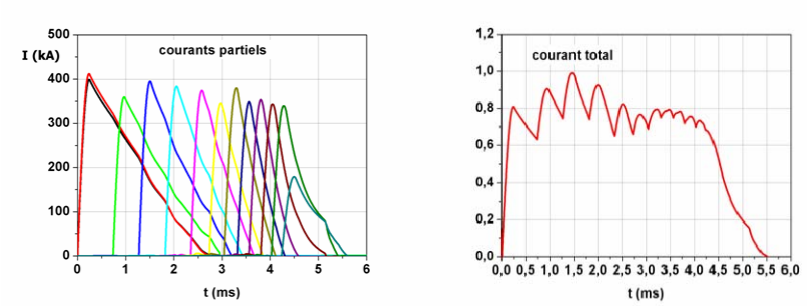

Figure 5: Typical current wave form generated by a capacitor bank connected to a railgun. Left: individual currents, right: total current

2.1. Mission

In recent years, the mesosphere and lower thermosphere (at altitudes between ~50 and 150 km) have attracted a considerable scientific interest because this altitude range hosts a wealth of fascinating geophysical phenomena like for example noctilucent clouds (NLC), polar mesosphere summer echoes (PMSE), mesosphere winter echoes, metal layers, etc. To mention only one interesting aspect, it is becoming clearer now that both NLC and PMSE are related to ice particles that exist in the extremely cold environment of the polar summer mesopause [8]. The polar summer mesopause is the coldest point in the entire Earth's atmosphere with temperatures reaching below ~130 K at ~88 km altitude [9-10]. It is these low temperatures that marginally allow ice particles to exist at altitudes between 80 to 90 km, i.e., 65 km higher than ordinary clouds down in the troposphere where the terrestrial weather takes place. Since the occurrence of ice clouds in this extreme environment is mainly temperature-controlled it has recently intrigued the scientific community to find indications that properties of these clouds (like brightness and occurrence frequency) seem to have changed over the past decades [11]. Right now there is an ongoing intense scientific debate whether these changes are either due to anthropogenic activity (i.e., anthropogenically enhanced atmospheric concentration of carbon dioxide is expected to lead to a cooling of the mesosphere and anthropogenically enhanced concentration of methane should lead to a larger water vapour supply at least in the stratosphere) or if it is just evidence of natural variability that we are far from quantitatively understanding at the current stage [12].

Hence, it is obvious that atmospheric altitudes between ~50 and 150 km are of significant scientific interest, however, when it comes to probe this region with sophisticated in situ techniques it turns out that this altitude range is extremely difficult to access at all. While atmospheric altitudes up to ~50 km can be reached with balloons, atmospheric density becomes too low at higher altitudes such that balloons do not

gain sufficient buoyancy to ascend further. Satellites on the other hand experience too strong drag and are hence limited to altitudes above say ~300 km. Hence, sounding rockets provide the only means to probe the mesosphere/lower thermosphere region in situ and so far there are no sufficiently precise remote sensing techniques (either ground based or satellite-borne) available that come only close to the accuracy of in situ measurements. Indeed, all modern satellite missions probing the mesosphere/lower thermosphere rely on the validation of their data products by sounding rocket measurements [13-14].

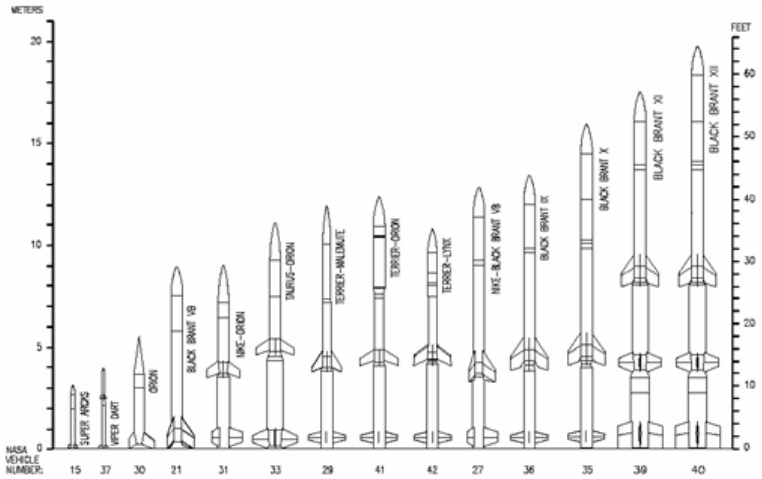

Figure 6: NASA sounding rockets [15].

Besides the two ESA sounding rockets, Texus and Maxus, which are intensively used for microgravity research, there are currently thirteen operational launch vehicles in the NASA Sounding Rocket program with different performance parameters and serving different needs. Extensive use is made of 20-30 years old military surplus motors in ten of the systems. All sounding rockets use solid propellant propulsion systems (**Fig. 6**), and most of them are unguided vehicles. During flight, the vehicles are imparted with a spinning motion to reduce potential dispersion of the flight trajectory due to vehicle misalignments. The obvious drawback of sounding rockets, however, is their poor price-performance ratio, i.e. usually one sounding rocket flight with typical costs of at least a couple of 100 k€ usually returns only one or two altitude profiles of the desired quantities (i.e., one on the ascent and one on the descent of the rocket trajectory). Hence, there exists a long history in the effort to miniaturize and/or simplify sounding rocket instrumentation in order to reduce the average cost of one measurement. One very successful example of such early efforts are so called meteorological rockets (=met-rockets) that have been launched by NASA already in the early 1960s [16-17] and that are still extensively used for both scientific investigations [9-10; 18] as well as for satellite validation purposes [13-14]. **Figure 7** sketched the measurement-principle of currently utilized met-rockets, here equipped with a so-called inflatable sphere, also called a "falling sphere". Another example for a recent successful miniaturization of an active sounding rocket experiment is the launch of a particle detector to probe ice particles in the upper polar summer mesosphere. This detector was first launched on a large two-stage sounding rocket with a Nike-Orion motor configuration [19] and then miniaturized and launched with a Viper-IIIA rocket motor that is usually utilized for the launch of meteorological payload systems [20].

Summarizing, the primarily market targeted for is the launch of scientific experiments for the research of the upper atmosphere, providing information on its chemical and physical decomposition. The corresponding requirements have been derived and evaluated from present and future planned miniaturized sounding rocket experiments. The payloads deployed are typically passive experiments like metallic spheres or aluminium chaff clouds, but also active instruments like particle detectors, dust probes etc as is shown in **Table 1**. A maximum payload mass of 1,000g with an associated volume of 270cm3 (a cylinder of 54cm length and 5cm diameter) is considered to cover all future applications incorporating a considerable margin. For active payloads a communication link will be available, which however reduces the size of the payload. All payloads are expected to be exposed at a maximum altitude of about 115km. In any case a strong adaptability exists to incorporate a wide range of future applications, varying in payload mass and target altitude.

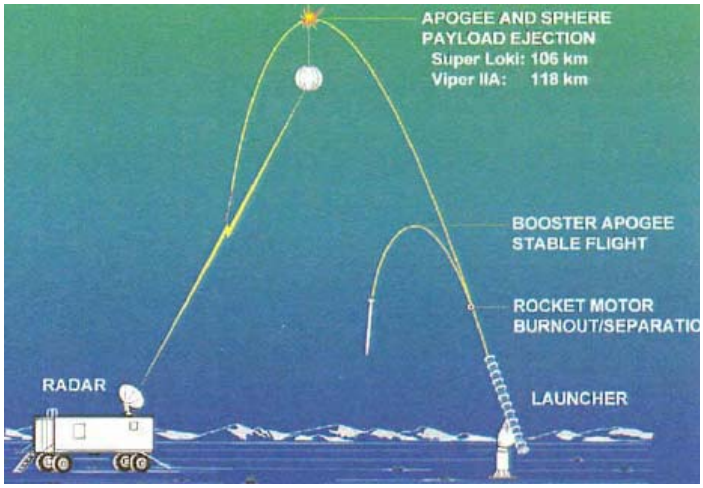

Figure 7: Operational principle of met-rocket measurements (courtesy Orbital Sciences).

Experiment	m [g]	Ø [cm]	l [cm]	
Falling Sphere	154	3.2	54.0	**Actual payloads**
Chaff Clouds	>100	3.2	54.0	
Photometer	600	4.0	54.0	**future payloads**
Dust Probes	600	4.0	54.0	
Part. Detector	< 500	2.0	54.0	
Spectrograph				
Laser Systems				
E-Field Booms				

Table 1: Payload requirements for present and future meteorological sciences.

The above mentioned dimensions are the main design drivers for the projectile since they have a direct influence on the layout of the gun. Higher launch masses require higher energy and consequently a longer railgun. Bigger diameters deteriorate the ballistic coefficient, thus enhancing the atmospheric drag,

increasing the heat load on the projectile and reducing the achievable target altitude. A preliminary mass budget has been calculated, assuming

- a payload mass including a release/inflation mechanism of 400g,
- a mass for the case, fins and insulation of the projectile of about 1.8kg and
- an additional mass of 1.7kg for both, the sabot and the armature

Consequently, the total mass to be accelerated by the railgun should not be greater than almost 4kg. This is considered as the present design baseline. A first proposed concept layout of the projectile is given in **Fig. 8**, including a cut section showing the payload cylinder and the ejection mechanism as well as tail fins to provide stability during flight. A nose cone with a spherical nosecap is selected. Behind the nosecap the contour is designed toward the power law with an exponent optimal for hypersonic velocities close to Ma = 6, which is the design Mach number. The nose-cone contour follows a tangential ogive shape. A smooth transition is obtained by means of a polynomial fit curve. The boat tail of the projectile is designed as a truncated reverse cone, resulting on a longitudinal cone angle which is lower than the critical angle of by which flow separation could be happen [21]. Four fins are positioned in crux configuration at the end of the cylindrical body. They have wedged trailing edges and blunted leading edges in order to alleviate the thermal loads and facilitate the manufacturing process.

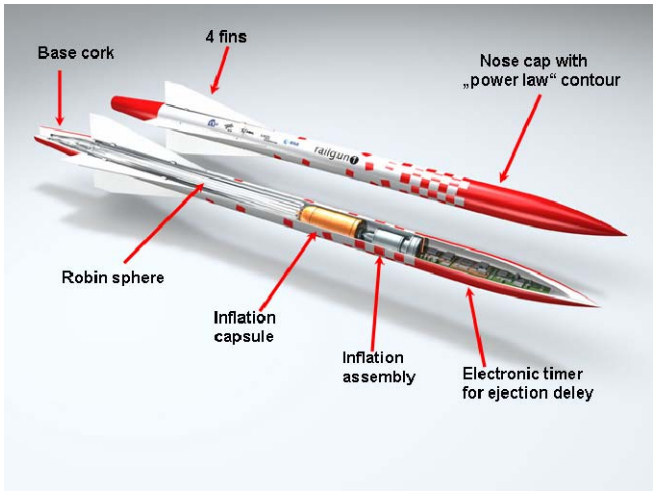

Figure 8: Conceptual layout for the railgun projectile showing payload and realise mechanism.

2.2. Launcher

The design of this entirely new launch system foresees the acceleration of lightweight and slim projectiles by an extension of the PEGASUS electromagnetic railguns currently under operation at the German-French Research Institute Saint-Louis. The PEGASUS (Program of an Electric Gun Arrangement to Study the Utilization in Systems) railgun facility was built in 1998 at ISL. As mentioned before, Fig. 4, it is a distributed energy storage railgun fed by a 10-MJ capacitor bank made of 200 modules of 50 kJ each. The facility was built to accelerate projectiles with a mass of 1 kg up to velocities greater than 2000 m/s with acceleration in the order of 70000 g's in the medium-caliber range (30, 40 and 50 mm). Tests are carried out with a 6-m-long and 40-mm-square-bore launcher tube currently connected to the PEGASUS facility.

The insulators between the Cu-Cr alloy rails consist of glass-fibre-reinforced plastic (GRP). The housing is made of insulated steel plates. The 200 energy modules are connected at 13 different locations along the tube. Each connection is fed by up to 16 coaxial cables.

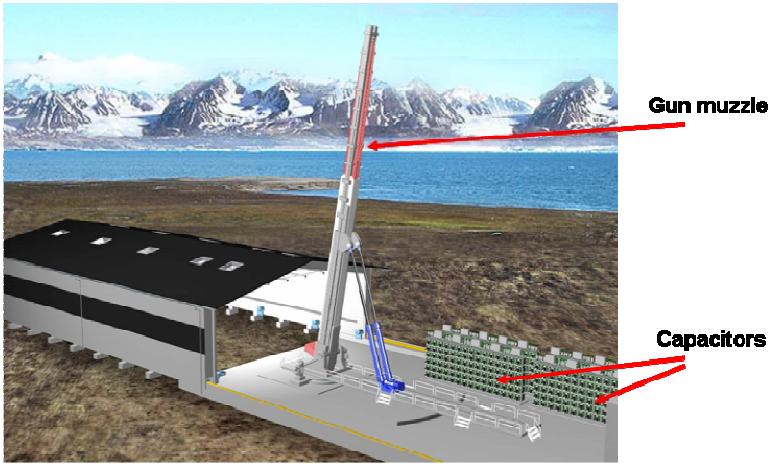

Figure 9: Artist impression of an operational railgun system.

The railgun itself should be 22m long and powered by a huge capacitor bank (**Fig. 9**). This technology is well-known and reliable. The scheme of the electrical circuit is shown **Fig. 10**. The capacitor bank is composed of 50 kJ modules. The main advantages of a modular energy supply are a high security standard since each Pulse Forming Unit (PFU) is disconnected from the next one; a good reliability; a high flexibility since an arbitrary total current pulse can be formed by choosing the triggering instant for each PFU; an enhanced overall efficiency of the railgun and also the possibility of using semiconductor switches, as the current and current rate for each module are limited to moderate values far below the critical ratings of the SCRs. The power supply is arranged along the launcher. The length of the cable connecting each 50-kJ-module to the railgun is assumed to be constant and equal to 10 m. The distribution of the current injections along the barrel allows a smooth variation of the mean acceleration.

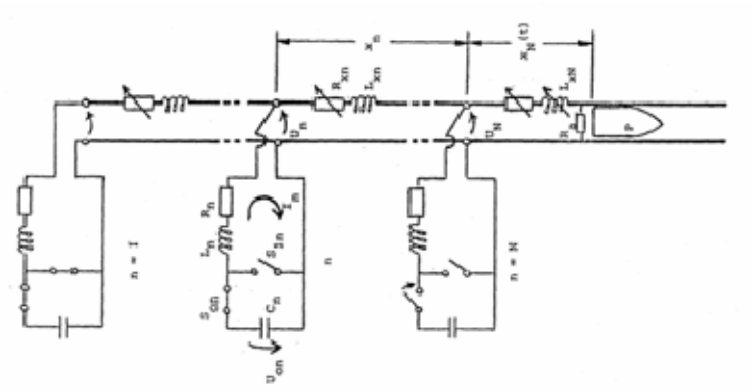

Figure 10: Schematic diagram of the railgun electric circuit.

The number of the stages, feeding each current injection, the number of modules per stage and the position of the current injections are varied in order to obtain high overall efficiencies. The stored energy of 32MJ will be delivered within 21ms to the rails, thus resulting in a power of 1.5GW. High-performance semiconductors will switch overall mean currents of 1.3 MA at a voltage of 10kV. A 1m long and 2.2kg heavy projectile will be accelerated at about 13,000g to hypersonic speed (Mach 6.2). It will reach the target altitude of 115km in less than 3 minutes during a ballistic flight, where the payload will be ejected (**Figs. 11**).

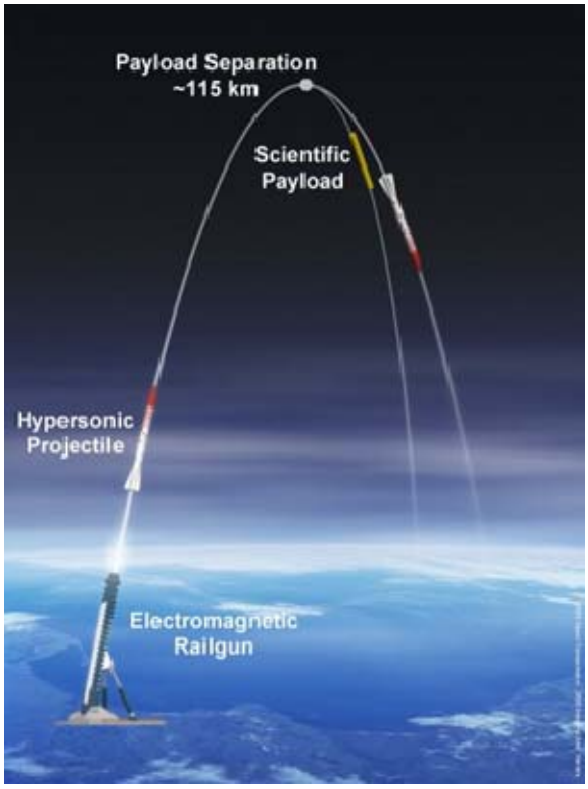

Figure 11: Typical suborbital mission profile.

The purpose of the following part of the lecture is to demonstrate that a design of a non propelled projectile to be launched by a rail gun in suborbital mission can be achieved with today available technologies making it not only feasible but also affordable. Here the aerodynamic, flight mechanic and thermal issues for such projectiles are presented and discussed.

2.2.1. Projectile

One of the main engineering tasks of a railgun launch system is the design of the so-called "Integrated Launch Package", which consists of the hypersonic projectile, an additional support structure for the stabilisation of the projectile during the acceleration in the barrel (sabot) and brush armature, which incorporates conductive wires in an insulating body to shortcut the currents of the two rails. In particular the harsh environmental conditions have to be reflected by the projectile's design, as there are high mechanical loads due to the envisaged acceleration levels of 13,000g and high aerothermal loads due to

atmospheric density and hypersonic speed. In particular, for the estimation of the expected atmospheric losses three different parameters have to be considered in detail: (i) the ballistic coefficient, defined as the ratio of squared diameter over mass of the projectile. The maximum diameter is presently given by the physical constraints of the railgun itself, limiting it to a caliber of 120 mm. As the diameter corresponds directly to the dissipation of energy, a much small diameter of 50 mm has been taken into consideration, enabling the housing of the actual sounding rocket experiments. (ii) the drag coefficient, based in general on handbook methods and/or semi-empirical estimations [22]. Minimum wave drag can be achieved using nose cups contouring according to the "power law" [23]. For the transonic Mach number range the base drag can be interpolated from calculated base drag values for subsonic and supersonic flows while the skin friction can be determined using compressible equations from handbook methods [24]. As a result the total drag coefficient is build up as superposition of wave, base and skin friction drag. The hypersonic velocity at the exit of the gun is considered to be a great advantage, as the total drag coefficient decreases below a value of 0.1 for Mach number Ma $\geq$ 4. Furthermore, the mission profile shows that the projectile reaches transonic and subsonic velocities within a fly path segment near to the apogee point (approx. 115 km). At this altitude the aerodynamic drag can be neglected, although the drag coefficient value reaches its maximum in the transonic Mach number range. (iii) the zero angle of trajectory inclination θ. A high elevation angle of 80-85^0, typical for sounding rockets, limits the travel time in the very dense atmosphere but also takes into account safety aspects to achieve given drop zones of the launch sites.

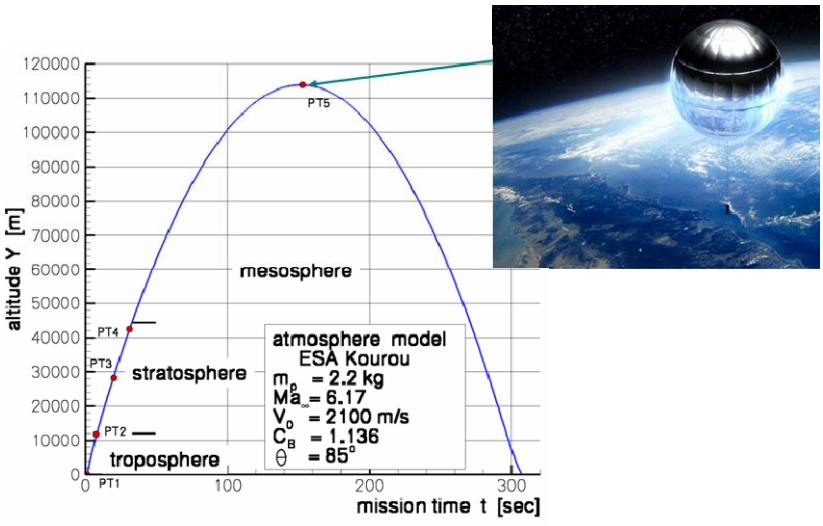

Figure 12: Mission profile.

Calculations have been performed to determine the ballistic flight paths as a function of the aerodynamic properties of the projectile as well as to predict the mechanical stresses of the projectile during the flight after being accelerated by the railgun. Different trajectories have been calculated to evaluate the maximum altitude reached by the projectile. As the apogee is strongly dependent on several parameters like mass and diameter of the projectile, i.e. the ballistic coefficient, starting velocity and zero angle of trajectory, a family of curves has been derived for a fixed projectile mass and a fixed elevation angle to determine the

sensitivity of the dimensioning. **Figure 12** shows the resulting ballistic flight-path for the proposed projectile and **Fig. 13** a zoom of the flight path in terms of time, for the first 30 seconds of flight. The projectile passes the troposphere and achieves the stratosphere in less then 7 sec (PT2) and it is already at 30,000 m after 20 sec (PT3). The figures also show that the projectile passes the densest atmosphere range, i.e. 42 km, after 29 sec (PT4). Finally, **Fig. 14** shows the trajectory Mach number development as a function of mission-time. It turns out that after the first 20 sec of flight the projectile experiences a strong deceleration as a consequence of the atmospheric drag. The loss of velocity is about $\Delta v = 830$m/s, i.e. 39 % of the launch velocity. This velocity losses continue up to the end of the stratosphere, where $\Delta v = 930$m/s, i.e. 44 % of the start velocity.

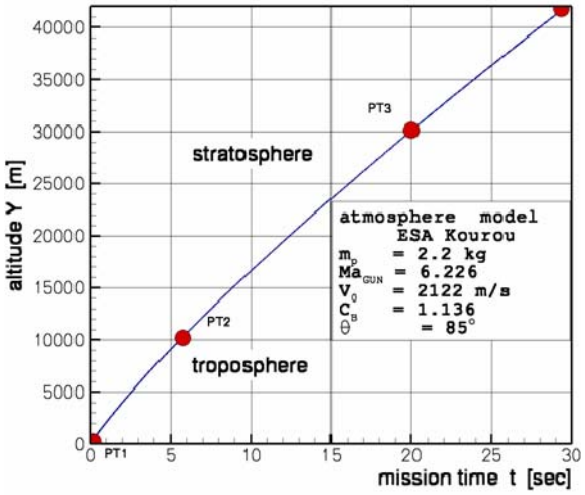

Figure 13: Zoom of the first 30 sec mission flight.

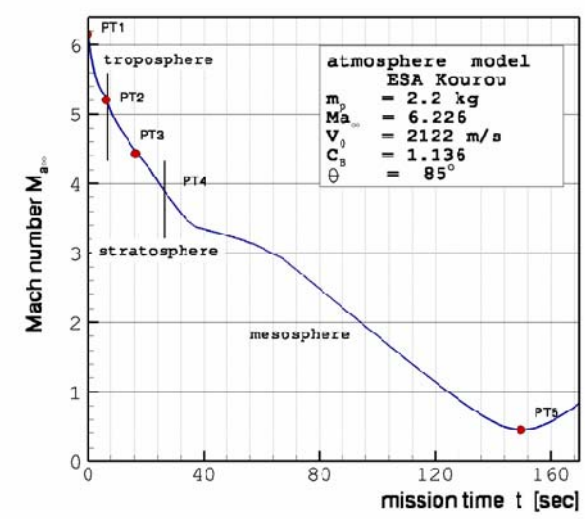

Figure 14: Mach number distribution along the trajectory ascent phase.

Since the projectile moves out the atmosphere in a very short time, it is important to quantify the impact that such decelerated motion may have on the projectile loads, in particular the thermal ones. Here CFD solutions representing real time trajectory points are required. The numerical solutions have benn obtained by coupling the Navier-Stokes TAU code of DLR with a 3DOF trajectory program. The data transfer between both programs is done by means of a BAHN_PYTHON_TAU interface (**Fig. 15**).

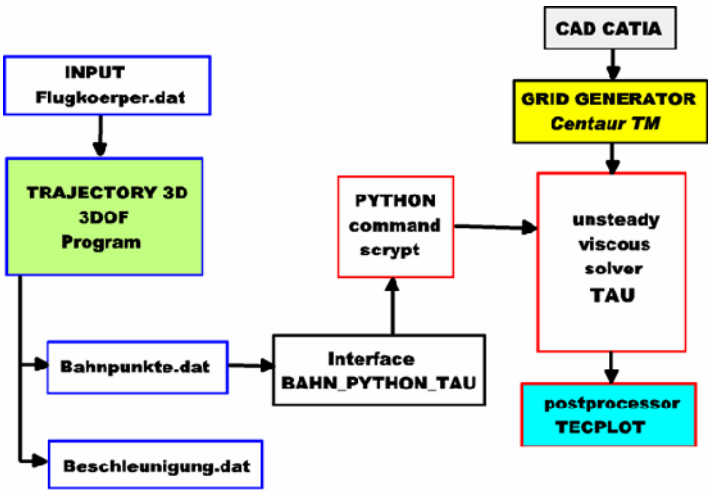

Figure 15: Computational strategy used for the CFD simulations along the flight path.

The 3DOF program is a 3 degree of freedom mass pointed method where all the forces like inertia, gravitation, drag and thrust are applied to a moving point in the space. The numerical integration is done by means of a Runge-Kutta technique. The method takes into account the effects of centrifugal and coriolis forces as well as wind profile. It considers also the changes of the gravitational constant with altitude, the effect of the earth rotation, the projectile initial velocity and its aerodynamic performance, in terms of lift and drag, the distribution of thrust over time, etc. Also, different atmospheric models can be selected by input. The TAU code is a finite-volume Euler/Navier-Stokes solver working with hybrid, unstructured or structured grids. The code is composed of three independent modules: a pre-processing module, a solver and a grid adaptation module. The flow solver is a three-dimensional finite volume scheme for solving the Reynolds-averaged Navier-Stokes equations. The temporal gradients are discretized using a multistep Runge-Kutta scheme. For accelerating the convergence to steady state a local time-stepping concept is employed. The calculation of the inviscid fluxes is performed using an AUSM or a Roe type 2nd-order upwind scheme. In TAU, there are several turbulence models available, ranging from 0 to 2 equations models and also Reynolds stress and Detached Eddy. For the present study the one-equation transport model according to Spalart and Allmaras [26] is selected. For time-accurate solutions a global as well as a dual time-stepping scheme is implemented. The dual time stepping scheme follows the approach of Jameson, where the Runge-Kutta scheme is slightly changed in order to avoid instabilities while dealing with small physical time-steps. The time discretization can be chosen to be first, second or third order (where a higher order implies increased overhead).

To compute the aerothermal loads the following assumptions have been done:

- In aerodynamics, unsteady phenomena are generated among others through shock boundary layer interactions, boundary layer separation, unsteady shock motions, vortical flows and transonic nonlinearities. For a projectile like the one considered here, unsteady flow conditions may be encountered on the nosecap, wings leading edges, wing-body junctions and at the boat tail. However, here it is assumed, that the projectile is absolutely stable and that the flight path is tangential to the trajectory, i.e. pitch, yaw and roll angles are equal to zero. Flow separations are neglected with exception of the after body which is considered non-critical. Furthermore, since the projectile starts from the railgun with hypersonic velocity and will continuously travel through the dense atmosphere at such speed, transonic unsteady effects are excluded from the analysis. Also aerolastic effects are neglected since the projectile's body is considered rigid. It turns out that as potential source of flow unsteadiness shock-wave boundary-layer interactions phenomena and projectile deceleration have to be considered only. Furthermore, since such phenomena are of short duration they are referred as transient or pseudo-unsteady for the present study.
- Absence of ablation and gas radiation is assumed. Also the interaction effects between the flow and the structure are not considered and therefore the related heat fluxes stored by the structure and the conductive heat flux, orthogonal to the surface, are not taken in account. In that case the heat balance equation reduces to only two terms, i.e. heat convection and heat radiation from the surface only.

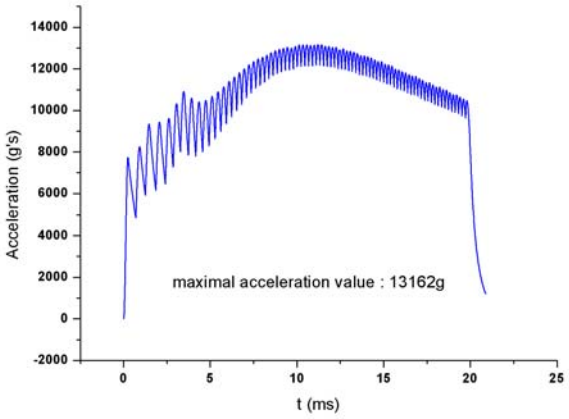

Figure 16: Projectile acceleration in the railgun tube.

- Within the first 20 ms the acceleration of the projectile in the gun tube will reach high values (**Fig. 16**). This acceleration is not uniform but dynamic with a frequency in the vicinity of the 1 kHz and close to the launch point, with amplitude of more than 1000 g. While the absolute mean value of the acceleration in the railgun tube is ~10,000g, a maximum acceleration value of 13,162g is achieved after 10 ms from launch. But once the projectile moves out of the railgun, air drag and gravitation will suddenly decelerate it. While the influence of the Earth gravitation is approximately constant and equal to 1g, the deceleration due to air drag has a maximum already at the railgun exit (**Fig. 17**).

Indeed, after 6 seconds of free flight, the projectile acceleration reduces to 5g and after 20 sec down to 1g, while the projectile is already at 30km altitude. It turns out that with the exception of the first few milliseconds inside the gun, the projectile deceleration is moderate and after 20 sec flight negligible.

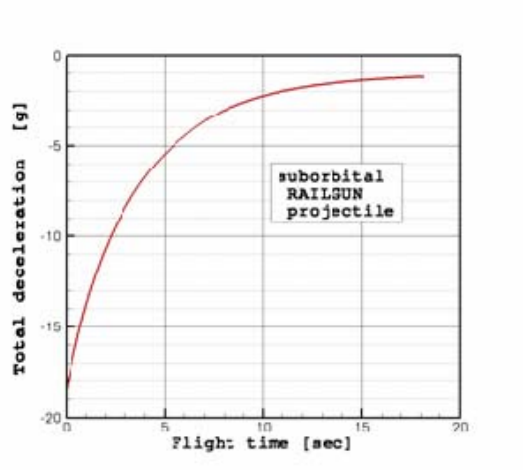

Figure 17: Projectile deceleration due to air drag and gravity forces.

- In hypersonic regime there are only few methods, all of them semi-empirical, for predicting turbulent/laminar flow transition. One of the most used is that from Bowcutt and Anderson [27]. Based on this criteria it is found that the transition Reynolds number is in the vicinity of Re=2.9 million (**Fig. 18**), a Reynolds number value which is firstly reached at an altitude of 27 km. At this altitude the heat loads and surface temperature of the projectile are no more critical.

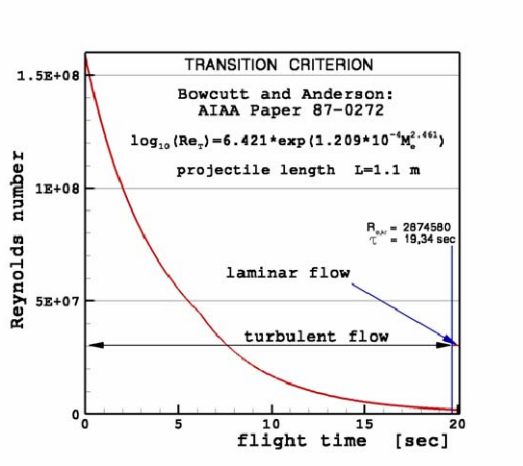

Figure 18: Occurrence of turbulent-laminar transition flow on projectile surface.

- As a first approximation it is assumed that the surface temperature of the projectile when it leaves the gun is 298 K (cold wall) and the acceleration due to the Lorentz force drops to zero. The launch

velocity is v_o= 2122 m/sec and the corresponding mach number Ma= 6.226. The total pressure is p_0 = 50.7 bar and the atmospheric conditions are given for an altitude of 1 m above sea level. A surface emission coefficient of ε = 0.85 is considered.

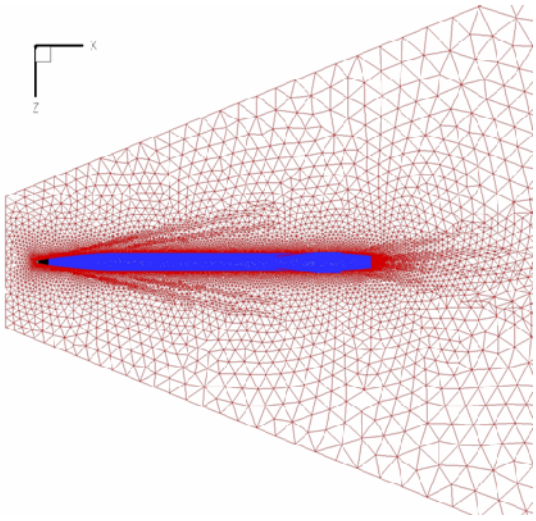

Figure 19: CFD grid with 7.5 millions hybrid elements.

For the CFD solutions the projectile's surface has been divided up into four blocks resulting in a grid of totally 8.6 millions cells, 52% of them in the prism layer (**Fig.19**). In order to draw an upper boundary of the expected thermal loads, some steady state solutions for selected trajectory points have firstly been obtained for zero angle of attack, neglected spinning, i.e. roll angle equals zero, assuming full catalytic surface, turbulent and laminar flow, radiation-adiabatic wall as well as constant wall temperature. The numerical error has been assessed using two grids of different density: 7.5 and a 8.6 million elements and also comparing the CFD values with those obtained by means of the Fay-Riddell formulation. The results show an agreement within 5 % or less (**Fig. 20**).

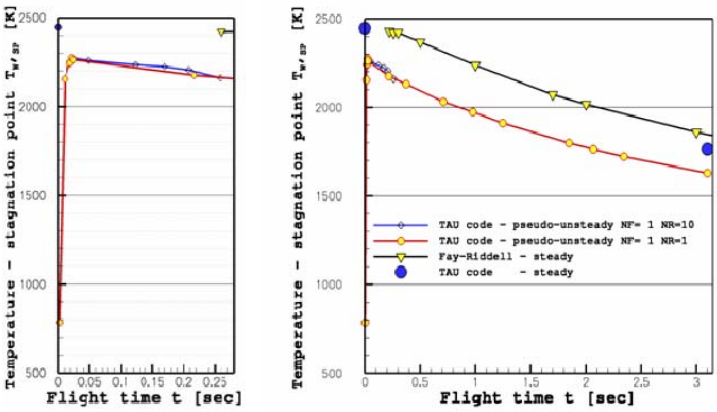

Figure 20: Transient temperature at the stagnation point after 27 ms (left) and 3 sec (right).

Since real-time unsteady computations are highly demanding on computational resources and computing time, only the first three seconds of flight have been considered. Concerning the thermal loads, this time interval is the most critical one since both, the projectile velocity and the air density exhibit the largest values. In order to achieve a high degree of accuracy while keeping computational efficiency, the computational time step shall increase as the time flight increases, while the solutions performed with different time steps shall compare rather good. This strategy has here been implemented subdividing the time domain in three segments: a one from gun exit to 0.0258 sec flight time, Mach range 6.22 <Ma< 6.217; a second one from gun exit to 0.97 sec of flight time, Mach range 6.22 <Ma< 5.918. For this interval the time step for the trajectory calculation is 10 time larger than the relaxation time-step for the CFD and equal to physical time step. The time step is varying along the trajectory between 0.0155 to 0.02638 sec.; and finally from gun exit to 3.1 sec flight time, Mach range 6.22 <Ma< 5.5. The time step for the trajectory calculation is varying from 0.0155 to 0.02638 sec. The number of iterations for each relaxation step is 500. **Table 2** displays the computational strategy and the required effort to obtain the solutions.

Nr.	Mach number Ma range	Calculated number of trajectory points	Time steps $\tau_{TR} = \tau_{Ph}$ [sec]	Number of relaxation time steps	Number of relaxation iterations	Calcul. flight time [sec]	Calcul. comp. Time [days]
1	6.226– 6.217	2	0.00248	10	500	0.0258	4.06
2	6.226– 5.918	48	0.0155 to 0.0264	10	500	0.258	35
3	6.226 – 5.5	136	0.0155 to 0.0264	1	500	3	77

Table 2: Time dependencies for carried coupled simulations on a 64bit workstation Siemens-Fujitsu with dual AMD OPTERON processors.

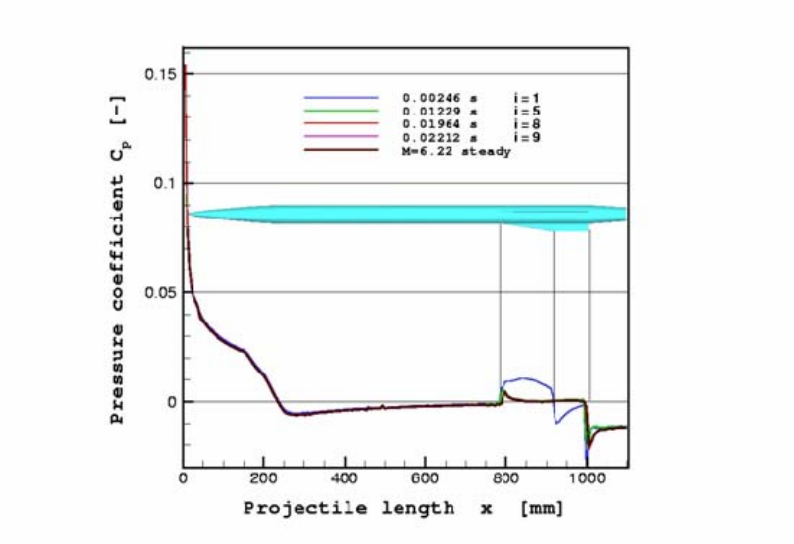

Figure 21: Longitudinal transient Cp distribution in the first 22 ms.

The results show that the pressure distribution achieves the steady state condition already in a few milliseconds, whereas the area of the fins requires a longer time, i.e. 22 ms (**Fig. 21**). The CFD simulations also show that within the first 20 ms the surface temperature achieves its maximum values (**Fig. 22**). Highest heat loads and temperatures occur, as expected, on the nosecap, leading edges of fins and body-fin junctions. As the projectile continues its flight, the surface temperature reduces to levels close to steady state. In the course of time the heat fluxes and surface temperatures, after they have reached their maximum in the first milliseconds of flight, decreases within the first 3 seconds to levels acceptable for a number of standard aerospace materials. Furthermore, the comparison between the pseudo-unsteady solutions with the steady one indicates a lower heating on the projectile front part during the transient motion but a moderate larger heating on fins and aft part, with temperature variations in the order of 50 to 100 K. Only at the stagnation region the differences are larger, exhibiting the transient solution almost 180 K less than the steady state case. Beside the potential impact of the numerical error that usually exhibits each solution at the stagnation point, there is a physical explanation for the observed difference: In the first few seconds of flight the projectile experiences a large deceleration and hence the bow shock moves continuously upstream, i.e. away from the nosecap, having no steady condition. After 3.1 sec of flight time (Ma=5.5) only moderate differences are observed (**Fig.23**).

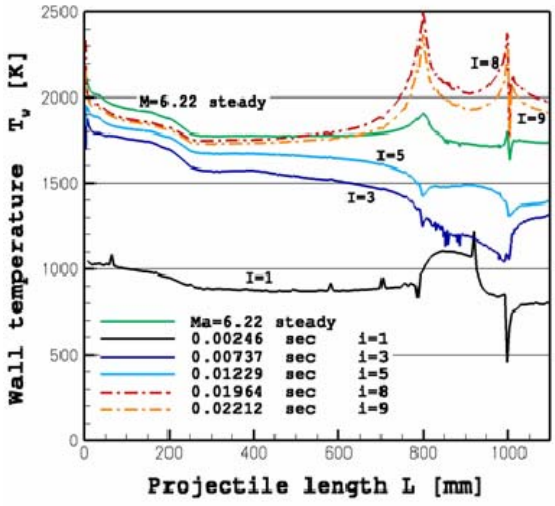

Figure 22: Longitudinal transient temperature distribution in the first 22 ms.

It turns out that due to the expected limited mission-time of two minutes, any environmental condition that the projectile may experience during launch and free flight can be handled with today's available materials and knowledge. Non-exotic materials, which are inexpensive and easy to work, may be chosen to handle the expected temperatures and mechanical loads. Metals and/or composites for the nose cone and thermoplastics for the case combined with stiffened insulation to support the entire structure and to protect the payload may be used.

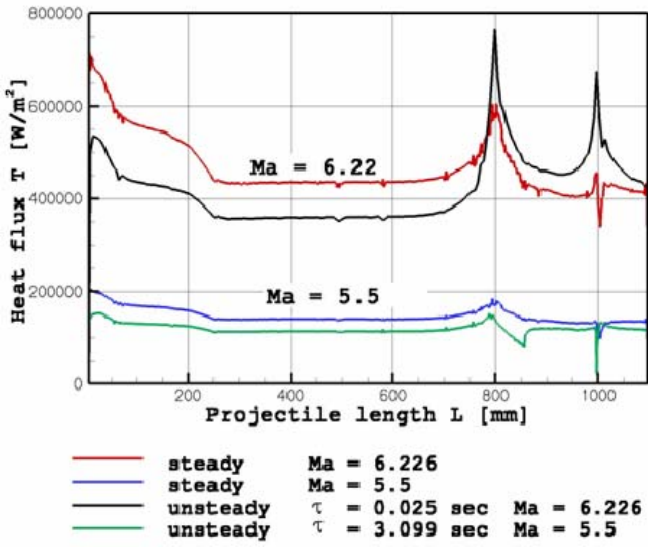

Figure 23: Longitudinal heat flux distribution by means of steady and transient computations.

3. Summary

The main focus of this lecture was the launch of hypersonic projectiles, accelerated by an electromagnetic railgun, as cost-effective platform for hypersonic and atmospheric experiments. As a very promising result it was shown, that with today‘s state of the art technology it is feasible to develop a projectile accelerated by an electromagnetic railgun to hypersonic speeds (v_o=2100m/s), carrying along a payload of 0.4 kg to an target altitude of 115 km. No major issues have been identified which cannot be implemented. Based upon today’s knowledge and the use of already existing potential key technologies, a launch system can be made available for the science user groups within the next few years with a minimum development risk. Indeed, the electromagnetic railgun parameters derived are based upon the long-lasting experience in developing and operating electromagnetic railguns at ISL. The railgun-version required for the launch of a 4 kg projectile is about four-times the current size of the facility actually operated by ISL. The thermal and mechanical loads acting on the projectile during the initial acceleration and the ballistic flight have been estimated and are considered decent showing that non-exotic and non-expensive materials may be used for later implementation and production. Even the projectile will experience a maximum acceleration of about 13,000 g's within a time-period of less than 21 ms, former studies for a wide variety of electronic components shown that they qualify for even higher acceleration levels up to 50,000g's or more, thus enabling sophisticated electronic payloads.

The envisaged reduction of the launch cost per probe is significant and may further enhance the competitiveness of the railgun system. The recurring costs of one probe including the supporting equipment like armature and sabot may be similar to those of the Martlet-2 series, i.e. in the order of 1/4 - 1/5 of the conventional small sounding rockets. Additional costs will for sure occur due to the operation and maintenance of the entire railgun system. Also for the users there are particular positive implications since the envisaged low launch price allow a drastic increase of in-situ measurements within the same given science budgets and also allow further cost savings due to the handling of non-hazardous cargo.

While the current design of the hypersonic projectile guarantees the accommodation of any existing and future meteo-payloads, thus exceeding the capability of any existing conventional small rocket system, in general the railgun launch system has the growth capability to cover all future envisaged passive and active meteorological instrumentation's, but in all cases they have to be adapted to high acceleration levels.

References

[1] McNab, I.R., *Launch to Space with an Electromagnetic Railgun*, IEEE Trans. On Magnetics 39 (2003)295.

[2] *Electro-Magnetic Rail Gun -Space Application* - DaimlerChrysler Aerospace Final Report, ESA Contract 13420/99/NL/MV, May 2000.

[3] Meier, T.A., *Assessment of Unconventional Space Transport System Candidates*, ESA-ESTEC/IMT-TSA, 27.10.1997.

[4] Feasibility Study of Gun Launch to Orbit (GL TO) for Small Payload Mass, TNO Report PML 1999-C60, September 1999.

[5] Behrens, J., Lehmann, P., Longo, J., Božić, O., Rap, M., Conde Reis, A., *Hypersonic and Electromagnetic Railgun Technology as a Future Alternative for the Launch of Suborbital Payloads*, Proceedings of the 16th ESA Symposium on Rockets and Balloon Programmes, St. Gallen, Swizerland, 2003.

[6] www.astronautix.com

[7] Lehmann, P., *Overview of the Electric Launch Activities at The French-German research Institute of Saint-Louis (ISL)*, IEEE Transactions on Magnetics 39 (2003) 24-28.

[8] Rapp, M., Lübken, F.-J., Blix, T., *The role of charged ice particles in the creation of PMSE: A review of recent developments,* Adv. Space Res., 31(9), 2033 - 2043, 2003.

[9] Lübken, F.-J., *Thermal structure of the Artic summer mesosphere*, J. Geophys. Res., 104, 9135-9149, 1999.

[10] Lübken, F.-J., Jarvis, M.J., Jones, G.O.L., First in situ temperature measurements at the Antartic summer mesopause, Geophys. Res. Lett., 26, 3581-3584, 1999.

[11] Thomas, G., *Are noctilucent clouds harbigers of global change in the middle atmosphere?*, Adv. Space Res., 31, 2003.

[12] Von Zahn, U., *Are Noctilucent clouds truly a Miner's canary of global change?*, EOS Transactions of the American Geophysical Union, 84(28), 261-268, 2003.

[13] Grossmann, K.U.D., Offermann, D., Gusev, O., Oberheide, J., Riese, M., Spang, R., *The CRISTA-2 Mission*, J. Geophys. Res., 107(D23), 8173, doi:10.1029/2001JD000667, 2002.

[14] Remsberg, E. et al., An assessment of the quality of Halogen Occultation Experiment temperature profiles in the mesosphere based on comparisons with Rayleigh backscatter lidar and inflatable falling sphere measurements, J. Geophys. Res., 107(D20), 4447, doi:10.1029/2001JD001521, 2002.

[15] *The Sounding Rocket Program Handbook*, NASA Goddard Space Flight Center, Wallops Flight Facility, Wallops Island, Virginia 2337, July 2001.

[16] Jones, L.M., Peterson, J.W., *Falling sphere measurements: 30 to 120 km*, Meteorological

Monographs, 8, 176-189, 1968.

[17] *Status of passive inflatable falling-sphere technology for atmospheric sensing to 100 km*, Proceedings of the Symposium Langley Research Center, Hampton, Virginia, September 23-24 1969, Scientific and Technical Information Division, Office of Technology Utilization National Aeronautics and Space Administration, Washington D.C., 1969, NASA SP-219.

[18] Schmidlin, F.J., *The inflatable sphere: A technique for the accurate measurement of middle atmosphere temperatures*, Geophys. Res., 96, 22, 673-22,682, 1991.

[19] Havnes, O., Troim, J., Blix, T., Mortensen, W., Naesheim, L.I., Thrane, E, Tonnesen, T., *First detection of charged dust particles in the Earth's mesosphere*, Geophys. Res., 101, 10,839-10,847,1996.

[20] Havnes, O., Brattli, A., Aslaksen, T, Singer, W., Latteck, R., Blix, T., Thrane, E., Troim, J., *First common volume observations of layered plasma structures and polar mesospheric summer echoes by rocket and radar*, Geophys. Res. Lett., 28, 1419-1422, 2001.

[21] Moore, F. G., *Approximate Methods for Weapons Aerodynamics*, AIAA Series Volumes: Progress in Astronautics and Aeronautics, ISBN 1-56347-399-2.

[22] Blagojevic, D., Jojic, B., Stefanovic, Z., Dervisevic, M., *Construction and calculation of unguided rocket – Part I: Aerodynamic and fly dynamic*, Saroj, Belgrad, 1977.

[23] Grodzovskogo, G.L. (Editor), *Aeromehaika sverhzvukogo obtekanija stepennoi formi*, Masinostroenie, Moskva, 1975.

[24] Jones, G.R., Swanson, N.J., Madura, D.L., Aerothermodynamic Issues Associated with Rail Gun Launched to Space Projectiles, AIAA/ASME 5th Joint Thermophysics and Heat Transfer Conference, Seattle, USA, AIAA Paper 90-1720, June 1990.

[25] Mack, A., Hannemann, V., *Validation of the Unstructured DLR-TAU-Code for Hypersonic Flows*, AIAA Paper 2002-3111, 2002.

[26] Deck, S., Duveau, P., d'Espiney, P.,Guillen, P., *Development and application of Spalart-Allmaras one equation turbulence model to tree-dimensional supersonic complex configurations*, Aerospace Science and Technology, Vol. 6, 2002, 171-183.

[27] Anderson, J. D. Jr., *Hypersonic and High Temperature Gas Dynamics*, McGraw-Hill Book Comp., Singapore, 1989.